Yan, W. M. & Li, X. S. (2011). *Géotechnique* **61**, No. 2, 95–106 [**doi:** 10.1680/geot.8.P.061]

A model for natural soil with bonds

W. M. YAN* and X. S. LI†

This paper presents a thermodynamically consistent constitutive model for natural soils with bonds. In the model, the free energy (the internal energy available to do work) is contributed partly by the so-called frozen or locked energy, whose evolution is assumed to be homogeneously related to the irrecoverable deformation. During loading, the bonds existing in the natural soil not only boost the dissipation rate but also liberate certain historically accumulated locked energy. Such effects, however, are diminished as loading proceeds and the bonds are destroyed. The novel aspect of the present model is that it accommodates both the Mohr–Coulomb and critical-state failure modes, and the two modes are unified through the evolution law of a thermodynamic force associated with the locked bonding energy. As compared with the classical Cam-clay models, the model contains two additional material constants, where one is proposed by Collins & Kelly to improve the shape of the yield surface, and the other is dedicated to bonding evolution. The calibration procedure for the material parameters is provided. The capability of the model is demonstrated by a series of model simulations on a hypothetical bonded soil under various triaxial loading paths, and the model response is also compared with representative testing results in the literature.

Cette communication présente un modèle constitutif à cohésion thermodynamique pour des sols naturels caractérisés par des liaisons. Dans ce modèle, à l'énergie libre (c'est à dire l'énergie disponible pour effectuer un travail) contribue en partie l'énergie figée, dont l'évolution est supposée être en rapport, de façon homogène, avec la déformation irrévocable. Au cours des charges, les liaisons présentes dans le sol naturel renforcent le taux de dissipation, tout en dissipant une certaine énergie figée qui s'est accumulée. Toutefois, ces effets diminuent au fur et à mesure des charges et de la destruction des liaisons. L'aspect nouveau du présent modèle est qu'il comprend à la fois les modes de déformation de Mohr–Coulomb et les modes d'état critique, ces deux modes étant unifiés par la loi de l'évolution d'une force thermodynamique associée à l'énergie de liaison figée. Par rapport aux modèles classiques de *CamClay*, ce modèle comprend deux constantes de matière supplémentaires, dont une est proposée par Collins & Kelly pour renforcer la forme de la surface d'élasticité, l'autre est consacrée à l'évolution des liaisons. La procédure de calibrage pour les paramètres de matériaux est fournie. La capacité de ce modèle est démontrée par une série de simulations de modèles sur un sol lié sous différents chemins de charge triaxiaux, et on en compare la réponse avec des résultats d'essais représentatifs existants.

KEYWORDS: clays; constitutive relations; numerical modelling; plasticity; shear strength; theoretical analysis

INTRODUCTION

The mechanical behaviour of natural soil is notably different from its remoulded counterpart (Burland, 1990; Leroueil & Vaughan, 1990; Burland *et al.*, 1996; Callisto & Calabresi, 1998; Gasparre *et al.*, 2007). During isotropic or K_0 compression, natural clays show a stiffer (lower compressibility) response than their corresponding reconstituted sediments up to a higher pressure, as shown schematically in Fig. 1(a). This indicates that, while a low compressibility is maintained, a natural soil can sustain a higher overburden pressure than its reconstituted counterpart. Further increase of this pressure results in a sharp yield point, after which the compression curve drops towards and eventually merges with the compression line of the reconstituted specimen (sometimes referred to as the intrinsic compression curve). Natural clays in general have a true cohesion arising from the geological processes, with which the specimen can stand at a zero confining pressure. This strength component, however, will be destroyed by loading, often leaving a distinct peak in the shear stress–strain curve, as shown in Fig. 1(b). It is generally accepted that there are bonds between natural clay grains, and it is these bonds that are responsible for the aforementioned observations.

Large varieties of soil constitutive models, including the well-known Cam-clay models, have been formulated since the development of critical-state soil mechanics (Roscoe *et al.*, 1958; Roscoe & Schofield, 1963; Roscoe & Burland, 1968; Schofield & Wroth, 1968). However, critical-state theory is applicable only to reconstituted clays in which bonding or true cohesion does not exist (Schofield, 1998, 2005, 2006). In this regard, it is understood that the strength of a reconstituted soil comes from internal friction and interlocking/dilation (Taylor, 1948). For a soil being distorted appreciably, interlocking (if any) is lost, and the soil will fail in a pure frictional manner, in which shear deformation can be developed indefinitely. This is the well-known critical or ultimate state of a soil. For natural soils, the presence of intergrain bonds results in a true cohesion, which is a strength component in addition to those due to interlocking and friction. It is evident that the intergrain bonds will be shattered by loading (disturbance) at a finite deformation; accordingly, true cohesion (if any) must be destroyed before a critical state is attained, because the critical state could accommodate an indefinitely developed shear strain at a constant strength. This hypothesis is obviously consistent with the critical-state framework, within which the soil properties do not depend on intergrain bonds at all (Schofield, 2005). It follows that, if the true cohesion is destroyed well before the soil dilatancy vanishes, one should expect a failure mode qualitatively similar to its remoulded counterpart (critical-state failure), but the peak

Manuscript received 5 May 2009; revised manuscript accepted 11 December 2009. Published online ahead of print 17 August 2010. Discussion on this paper closes on 1 July 2011, for further details see p. ii.

* Department of Civil Engineering, The University of Hong Kong.
† Department of Civil and Environmental Engineering, Hong Kong University of Science and Technology.

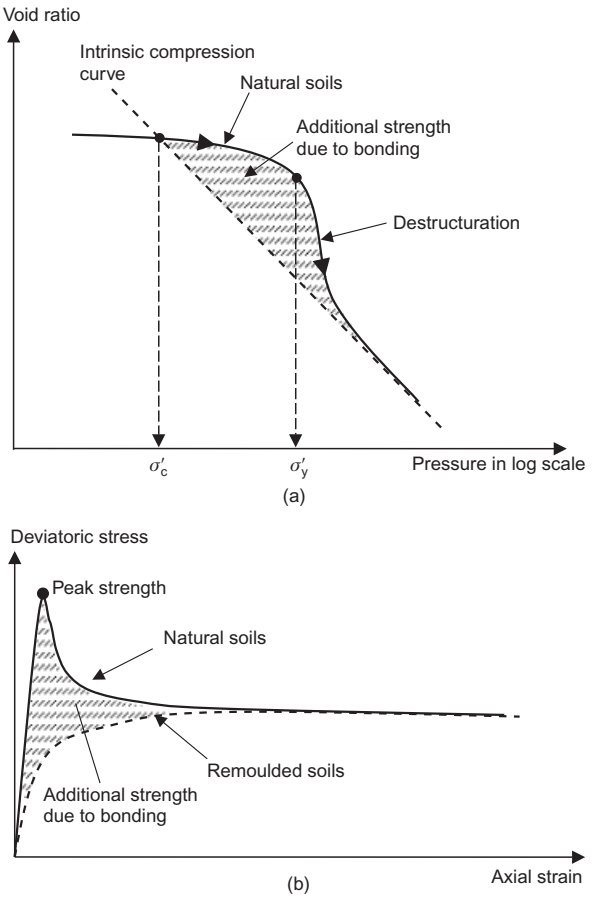

Fig. 1. Typical response of natural soil during compression: (a) isotropic or one-dimensional compression; (b) drained shearing

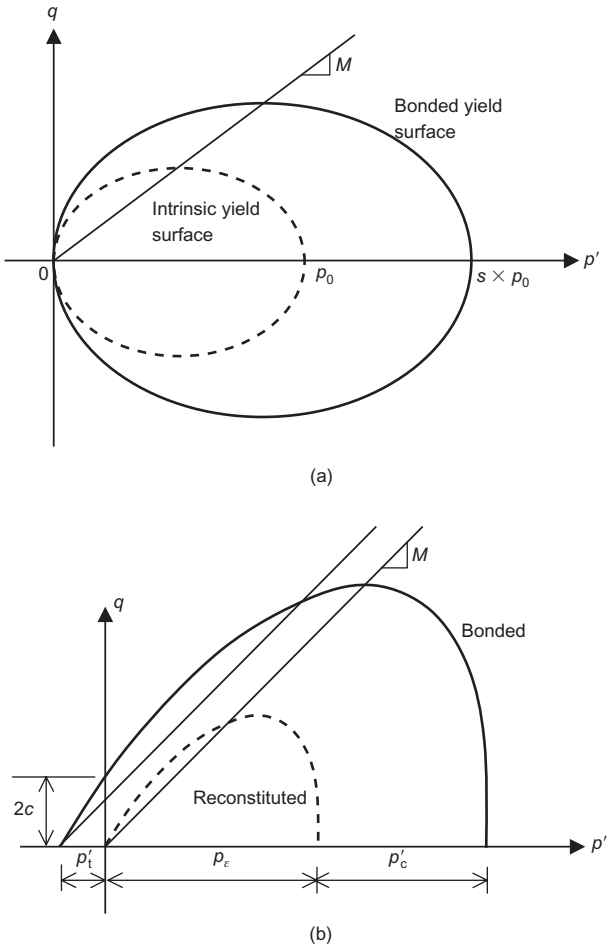

Fig. 2. Yield surface for bonded soil: (a) sensitivity surface (from Baudet & Stallebrass, 2004); (b) enlarged yield surface (from Yu *et al.*, 2007)

strength on the 'dry' side will depend not only on the soil density but also on the intergrain bonding. On the other hand, if a true cohesion still exists when the dilatancy approaches zero, then the shear resistance in that state will be contributed by both internal friction and cohesion, but not interlocking. As shear proceeds further, the remaining cohesion will be abruptly destroyed, because the frictional part of resistance, once it prevails, does not restrict further development of shear deformation. This type of failure satisfies the classical Mohr–Coulomb criterion, with which the soil behaves as a brittle material.

Recently, Baudet & Stallebrass (2004) and Yu *et al.* (2007), among others, extended the concept of critical-state soil mechanics to geomaterials with bonds. Following the sensitivity framework originally developed by Cotecchia & Chandler (2000), Baudet & Stallebrass (2004) employed a sensitivity parameter s to characterise an expanded yield surface, called the sensitivity surface. This surface stems from the origin of p–q space, and is s times larger than the intrinsic yield surface for fully remoulded states (Fig. 2(a)). The sensitivity surface shrinks gradually in the process of destructuration through an evolution law, by which $\dot{s}$ is related homogeneously to a plastic strain rate. This model has not taken into account the cohesion or tensile strength that is produced by intergrain bonds, and is not intended to make the ultimate states (the fully disturbed states) a critical state on a uniquely defined p–q–e critical-state line (where e is the void ratio). On the other hand, the model proposed by Yu *et al.* (2007) considers the true cohesion imparted by the bonds between natural soil grains. Two bond-related parameters, p_b and p_μ (denoted as by p'_t and p'_c respectively in their original paper), are introduced to define the size and location of the yield surface (Fig. 2(b)). The yield surface cuts the $p = 0$ axis with an intercept of $2c$, and therefore effectively represents true cohesion. The progressive bond degradation is modelled by evolution laws of p'_c and c, such that they both approach zero when the deformation approaches infinity. The model is not, however, intended to simulate the brittle mode of failure that is linked to an abrupt destruction of the true cohesion.

From the thermodynamics perspective (Collins & Houlsby, 1997; Houlsby & Puzrin, 2000; Collins & Kelly, 2002; Li, 2007a, 2007b), plasticity theory, on which most soil models are based, is a mechanistic framework that describes the dissipation process. As stated by Schofield (1998, 2005, 2006), the dissipation in critical-state theory is due only to internal friction, and not to cohesive or adhesive bonds between disturbed soil grains. It follows that, for natural soils with true cohesion, additional dissipation associated with interparticle bonds must be properly introduced; and when the soil becomes fully disturbed (destructured), the dissipation should merge into the classical critical-state framework: that is, the dissipation mechanism is frictional in nature, and is affected by interlocking (dilatancy). By taking fully destructured states as reference, one finds that bonding has two effects. First, because of bonding, the thermodynamic force conjugate with plastic deformation (dissipative deformation) in dissipation increases, which in turn promotes the dissipation rate (the dissipation per unit plastic deformation). Second, in its formation history, bonding accumulated a certain amount of energy that is locked in the intact soil structure. Once the soil is disturbed, accompanying plastic

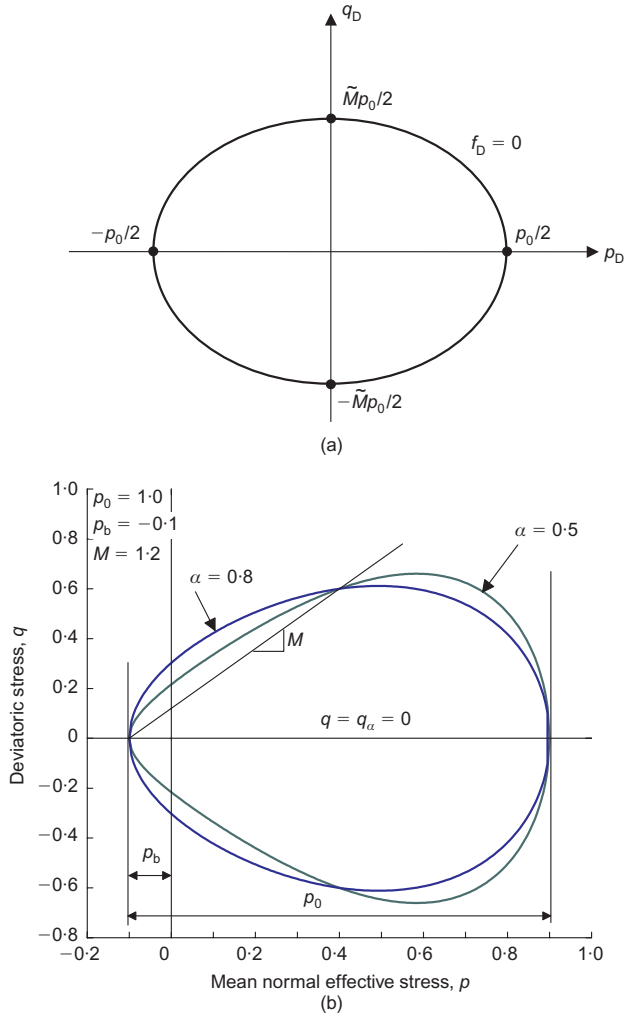

Fig. 3. Yield surface in: (a) dissipative stress space; (b) triaxial true stress space

deformation, this part of the locked energy is released, so that the soil gradually approaches more stable states (remoulded states).

In this paper, the aforementioned bonding effects are cast into the thermodynamics framework, and an elasto-plastic model consistent with the framework is presented. A calibration procedure is given with which all the material constants can be determined, based on conventional laboratory tests. The model simulations are then compared with available test results in the literature.

THERMODYNAMICS CONSISTENT PLASTICITY FRAMEWORK

The first law of thermodynamics expresses the principle of energy conservation. For a representative unit volume of soil skeleton, it can be written as

$$\mathrm{d}u = \boldsymbol{\sigma} : \mathrm{d}\boldsymbol{\varepsilon} + \delta Q \tag{1}$$

where u is the internal energy possessed by the element, $\boldsymbol{\sigma}$ is the effective stress, $\boldsymbol{\varepsilon}$ is the strain and Q is the heat entering the element. 'd' and 'δ' denote exact and inexact differentials respectively. As all the stresses in the present paper are effective stresses, the prime conventionally attached to effective stresses is omitted.

The second law of thermodynamics states the irreversibility of a process involving dissipation, which is written as

$$\theta\gamma = \theta \mathrm{d}s - \delta Q \geqslant 0 \tag{2}$$

where $\theta > 0$ is the absolute temperature, s is the entropy, and γ is the entropy production. Note that $\theta\gamma$ represents an infinitesimal change in dissipation that is never negative. Combining equations (1) and (2) yields

$$\mathrm{d}u = \boldsymbol{\sigma} : \mathrm{d}\boldsymbol{\varepsilon} - \theta\gamma + \theta \mathrm{d}s \tag{3}$$

where the part of the energy free to do work (the Helmholtz free energy) is

$$\psi = u - s\theta \tag{4}$$

and its increment under isothermal conditions ($\mathrm{d}\theta = 0$) is

$$\mathrm{d}\psi = \mathrm{d}u - \theta \mathrm{d}s = \boldsymbol{\sigma} : \mathrm{d}\boldsymbol{\varepsilon} - \theta\gamma \tag{5}$$

By additive decomposition $\mathrm{d}\boldsymbol{\varepsilon} = \delta\boldsymbol{\varepsilon}^{\mathrm{e}} + \delta\boldsymbol{\varepsilon}^{\mathrm{p}}$, where the superscripts e and p stand for elastic and plastic respectively; and taking plastic deformation as the dissipative kinematic measure, one has

$$\mathrm{d}\psi = \underbrace{\underbrace{\boldsymbol{\sigma} : \delta\boldsymbol{\varepsilon}^{\mathrm{e}}}_{\text{elastic energy}} + \underbrace{\boldsymbol{\alpha} : \delta\boldsymbol{\varepsilon}^{\mathrm{p}}}_{\text{locked-in energy}}}_{\text{stored energy}} + \underbrace{\underbrace{(\boldsymbol{\sigma} - \boldsymbol{\alpha}) : \delta\boldsymbol{\varepsilon}^{\mathrm{p}}}_{\text{dissipation in terms of macro-deformation}} - \underbrace{\phi}_{\text{dissipation in terms of internal rearrangements}}}_{0} \tag{6}$$

where $\boldsymbol{\alpha}$, $(\boldsymbol{\sigma} - \boldsymbol{\alpha}) \triangleq \boldsymbol{\sigma}_{\mathrm{D}}$ and $\phi = \theta\gamma$ are referred to as the back or shifted stress, the dissipative stress and the dissipation respectively. By assuming the dissipation $\phi = \phi(\boldsymbol{\sigma}_{\mathrm{D}}, \boldsymbol{\sigma}, \mathcal{H})$ with $\mathcal{H}$ denoting the material's internal structure, the balance of the dissipative stress work and internal dissipation results in a function

$$\begin{aligned} f_{\mathrm{D}} &= f_{\mathrm{D}}(\boldsymbol{\sigma}_{\mathrm{D}}, \boldsymbol{\sigma}, \mathcal{H}) \\ &= \boldsymbol{\sigma}_{\mathrm{D}} : \delta\boldsymbol{\varepsilon}^{\mathrm{p}} - \phi(\delta\boldsymbol{\varepsilon}^{\mathrm{p}}, \boldsymbol{\sigma}, \mathcal{H}) = 0 \end{aligned} \tag{7}$$

which is in fact a definition of the yield function in the dissipative stress $\boldsymbol{\sigma}_{\mathrm{D}}$ space. $\mathcal{H}$ is materialised by a set of internal variables, which are not necessarily state variables (Rice, 1971), in the sense that their values in a given state may be path-dependent. Based on the assumption of incremental linearity and the hypothesis of maximum dissipation rate, Ziegler (1983) obtained his famous orthogonality condition $\boldsymbol{\sigma}_{\mathrm{D}} = \partial\phi/\partial(\delta\boldsymbol{\varepsilon}^{\mathrm{p}})$, which maps into the dissipative stress space, yielding the associative flow rule

$$\delta\boldsymbol{\varepsilon}^{\mathrm{p}} = \langle L \rangle \frac{\partial f_{\mathrm{D}}}{\partial \boldsymbol{\sigma}_{\mathrm{D}}} \tag{8}$$

where L is a loading index, and $\langle\ \rangle$ are the McCauley brackets, such that $\langle L \rangle = L$ if $L \geqslant 0$, and $\langle L \rangle = 0$ otherwise. Clearly, by treating the back stress as a general function of stress and the material's internal structure, $\boldsymbol{\alpha} = \boldsymbol{\alpha}(\boldsymbol{\sigma}, \mathcal{H})$, one can express such a yield function in the actual stress space as

$$f = f(\boldsymbol{\sigma}, \mathcal{H}) \triangleq f_{\mathrm{D}}\left(\underbrace{\boldsymbol{\sigma} - \boldsymbol{\alpha}}_{\boldsymbol{\sigma}_{\mathrm{D}}}, \boldsymbol{\sigma}, \mathcal{H}\right) = 0 \tag{9}$$

It follows that the condition of consistency is given by

$$\begin{aligned} \mathrm{d}f = &\underbrace{\left(\frac{\partial f_{\mathrm{D}}}{\partial \boldsymbol{\sigma}_{\mathrm{D}}} - \frac{\partial f_{\mathrm{D}}}{\partial \boldsymbol{\sigma}_{\mathrm{D}}} : \frac{\partial \boldsymbol{\alpha}}{\partial \boldsymbol{\sigma}} + \frac{\partial f_{\mathrm{D}}}{\partial \boldsymbol{\sigma}}\right)}_{\partial f/\partial \boldsymbol{\sigma}} : \mathrm{d}\boldsymbol{\sigma} \\ &+ \underbrace{\left(\frac{\partial f_{\mathrm{D}}}{\partial \mathcal{H}} - \frac{\partial f_{\mathrm{D}}}{\partial \boldsymbol{\sigma}_{\mathrm{D}}} : \frac{\partial \boldsymbol{\alpha}}{\partial \mathcal{H}}\right)}_{\partial f/\partial \mathcal{H}} \delta\mathcal{H} = 0 \end{aligned} \tag{10}$$

which yields a generally non-associative flow rule and hardening laws depending on the evolution of the back stress $\boldsymbol{\alpha}$.

Because of incremental linearity, the change in internal variables can be written as $\delta\mathcal{H} = \langle L\rangle r$, with r functions of stress and material's internal structure in general. Therefore the condition of consistency can be written in the normal form

$$\mathrm{d}f = \frac{\partial f}{\partial \boldsymbol{\sigma}} : \mathrm{d}\boldsymbol{\sigma} - \langle L\rangle K_\mathrm{p} = 0 \tag{11}$$

where $K_\mathrm{p} = -(\partial f/\partial\mathcal{H})r$ is the plastic modulus.

Equation (7) shows clearly that the dissipation ϕ is not necessarily equal to the plastic work $\boldsymbol{\sigma} : \delta\boldsymbol{\varepsilon}^\mathrm{p}$. The dissipation is less than the plastic work if part of the work is stored as locked energy, and the dissipation is greater than the plastic work if previously locked energy is liberated. The latter applies to the process of destructuration, in which the bonding between clay grains is gradually destroyed. From the constitutive model point of view, this effect is reflected by the evolution of the back stress $\boldsymbol{\alpha}$, which approaches a limit when the bonds are completely destroyed and the material behaves as a remoulded soil. To be consistent with critical-state soil mechanics theory, such a limit must be reached at critical states where the p–q–e state falls onto a uniquely defined critical-state line. In addition, breaking bonding needs additional power and produces additional dissipation. This is reflected in equation (7) as a higher dissipation ϕ per unit plastic strain increment $\delta\boldsymbol{\varepsilon}^\mathrm{p}$. Again, as the interparticle bonds are gradually destroyed, ϕ eventually merges to its reference values for remoulded states including critical states.

One may therefore conclude that a constitutive model for natural soil with bonds can be built upon the basis of its remoulded counterpart (usually a critical-state model) by modifying the formulations of the dissipation and back stress, as well as their evolution laws (the hardening laws).

Assuming the hypoelastic relation $\mathrm{d}\boldsymbol{\sigma} = \boldsymbol{E} : \delta\boldsymbol{\varepsilon}^\mathrm{e} = \boldsymbol{E} : (\mathrm{d}\boldsymbol{\varepsilon} - \delta\boldsymbol{\varepsilon}^\mathrm{e})$ and recalling the flow rule, equation (8), one obtains by the standard procedure the loading index

$$L = \frac{(\partial f/\partial\boldsymbol{\sigma}) : \boldsymbol{E}}{(\partial f/\partial\boldsymbol{\sigma}) : \boldsymbol{E} : (\partial f_\mathrm{D}/\partial\boldsymbol{\sigma}_\mathrm{D}) + K_\mathrm{p}} : \mathrm{d}\boldsymbol{\varepsilon} \tag{12}$$

and the incremental stress–strain relationship

$$\mathrm{d}\boldsymbol{\sigma} = \left[\boldsymbol{E} - h(L)\frac{\boldsymbol{E} : (\partial f_\mathrm{D}/\partial\boldsymbol{\sigma}_\mathrm{D}) \otimes (\partial f/\partial\boldsymbol{\sigma}) : \boldsymbol{E}}{(\partial f/\partial\boldsymbol{\sigma}) : \boldsymbol{E} : (\partial f_\mathrm{D}/\partial\boldsymbol{\sigma}_\mathrm{D}) + K_\mathrm{p}}\right] : \mathrm{d}\boldsymbol{\varepsilon} \tag{13}$$

where $\boldsymbol{E}$ is the elastic stiffness tensor and $h(L)$ is the Heaviside function of L ($h(L) = 1$ if $L > 0$ and $h(L) = 0$ otherwise). Equations (12) and (13) are the classical results. The deliberation in this section simply reiterates the generality of the classical elasto-plastic framework, and provides physical interpretations for certain fundamental modelling ingredients.

TRIAXIAL MODEL

Following the above general framework, a specific model is developed in the triaxial space, which involves two stress invariants, $p = (\sigma_\mathrm{a} + 2\sigma_\mathrm{r})/3$ and $q = (\sigma_\mathrm{a} - \sigma_\mathrm{r})$, and two strain invariants, $\varepsilon_\mathrm{v} = \varepsilon_\mathrm{a} + 2\varepsilon_\mathrm{r}$ and $\varepsilon_\mathrm{q} = 2(\varepsilon_\mathrm{a} - \varepsilon_\mathrm{r})/3$, where the subscripts a and r stand for axial and radial respectively.

Hypoelastic relations

The elastic response is described by the commonly used incremental relations

$$\begin{cases} \mathrm{d}p = K\mathrm{d}\varepsilon_\mathrm{v}^\mathrm{e} = \dfrac{\upsilon_0 p}{\kappa}\mathrm{d}\varepsilon_\mathrm{v}^\mathrm{e} \\ \mathrm{d}q = 3G\delta\varepsilon_\mathrm{q}^\mathrm{e} = \dfrac{9K(1-2\nu)}{2(1+\nu)}\delta\varepsilon_\mathrm{q}^\mathrm{e} = \dfrac{9\upsilon_0 p(1-2\nu)}{2\kappa(1+\nu)}\delta\varepsilon_\mathrm{q}^\mathrm{e} \end{cases} \tag{14}$$

where K and G are the elastic bulk and shear moduli respectively; ν and κ are two material constants; and υ_0 is a reference specific volume at which the volumetric strain $\varepsilon_\mathrm{v} = 0$. Note that the shear modulus so defined depends on the mean normal stress p, making equation $(14)_2$ hypoelastic. On the other hand, equation $(14)_1$ is integrable, making the relationship between p and $\varepsilon_\mathrm{v}^\mathrm{e}$ exactly elastic (path independent). Consequently, the plastic volumetric strain $\varepsilon_\mathrm{v}^\mathrm{p}$ is a state variable too.

Yield function

Equation (7) cast into the triaxial space reads as

$$\underbrace{(p - p_\alpha)}_{p_\mathrm{D}}\mathrm{d}\varepsilon_\mathrm{v}^\mathrm{p} + \underbrace{(q - q_\alpha)}_{q_\mathrm{D}}\delta\varepsilon_\mathrm{q}^\mathrm{p} = \phi \tag{15}$$

where p_α, q_α, p_D and q_D are the back and dissipative stresses respectively; and $\mathrm{d}\varepsilon_\mathrm{v}^\mathrm{p}$ and $\delta\varepsilon_\mathrm{q}^\mathrm{p}$ are the plastic volumetric and deviatoric strain increments respectively. The Cam-clay type dissipation function (Roscoe & Burland, 1968; Collins & Kelly, 2002)

$$\phi = \frac{p_0}{2}\sqrt{(\mathrm{d}\varepsilon_\mathrm{v}^\mathrm{p})^2 + \tilde{M}^2(\delta\varepsilon_\mathrm{q}^\mathrm{p})^2} \tag{16}$$

is adopted in the present study, where the parameter $\tilde{M}$ is a modified version of the Cam-clay constant M (Collins & Kelly, 2002). For simplicity, the presentation is limited to isotropic material only: thus $q_\alpha = 0$ and $q_\mathrm{D} = q$. It follows that we have

$$p_\mathrm{D}\mathrm{d}\varepsilon_\mathrm{v}^\mathrm{p} + q\delta\varepsilon_\mathrm{q}^\mathrm{p} = \frac{p_0}{2}\sqrt{(\mathrm{d}\varepsilon_\mathrm{v}^\mathrm{p})^2 + \tilde{M}^2(\delta\varepsilon_\mathrm{q}^\mathrm{p})^2} \tag{17}$$

which yields

$$p_\mathrm{D} = \frac{p_0 D}{2\sqrt{D^2 + \tilde{M}^2}} \tag{18}$$

and

$$q = \frac{p_0\tilde{M}^2}{2\sqrt{D^2 + \tilde{M}^2}}\mathrm{sgn}(\delta\varepsilon_\mathrm{q}^\mathrm{p}) \tag{19}$$

where $D = \mathrm{d}\varepsilon_\mathrm{v}^\mathrm{p}/|\delta\varepsilon_\mathrm{q}^\mathrm{p}|$ is the dilatancy. Combining equations (18) and (19) yields an elliptic yield surface (Fig. 3(a)) in the dissipative stress space, as

$$f_\mathrm{D} = p_\mathrm{D}^2 + \frac{q^2}{\tilde{M}^2} - \frac{{p_0}^2}{4} = 0 \tag{20}$$

Following Li's (2007b) proposition, by defining

$$p_\alpha = \frac{p_0}{2} + p_\mathrm{b} \tag{21}$$

and

$$\tilde{M} = \sqrt{M^2\left[\alpha + (1-\alpha)\frac{2(p - p_\mathrm{b})}{p_0}\right]^2} \tag{22}$$

the yield function in the actual stress space can be written as

$$f = f(p, q, p_0, p_b) = M^2\left[4(1-\alpha)^2\frac{(p-p_b)^4}{p_0^2} - 4(1-3\alpha+2\alpha^2)\frac{(p-p_b)^3}{p_0} - \alpha(4-5\alpha)(p-p_b)^2 - \alpha^2(p-p_b)p_0\right] + q^2 = 0 \tag{23}$$

which yields the partial derivatives

$$\begin{cases} \dfrac{\partial f}{\partial p} = M^2\left[16(1-\alpha)^2\dfrac{(p-p_b)^3}{p_0^2} - 12(1-3\alpha+2\alpha^2)\dfrac{(p-p_b)^2}{p_0} - 2\alpha(4-5\alpha)(p-p_b) - \alpha^2 p_0\right] \\ \dfrac{\partial f}{\partial q} = 2q \\ \dfrac{\partial f}{\partial p_0} = M^2\left[-8(1-\alpha)^2\dfrac{(p-p_b)^4}{p_0^3} + 4(1-3\alpha+2\alpha^2)\dfrac{(p-p_b)^3}{p_0^2} - \alpha^2(p-p_b)\right] \\ \dfrac{\partial f}{\partial p_b} = -\dfrac{\partial f}{\partial p} \end{cases} \tag{24}$$

In equation (23), p_0 and p_b define the size and location of the yield surface respectively, as shown in Fig. 3(b); M and α are two material constants, in which M is the classical Cam-clay parameter (the critical stress ratio), and α describes the shape of the yield function (Collins & Kelly, 2002). The introduction of α distorts the yield surface from an ellipse to a teardrop shape (Fig. 3(b)), which provides an additional flexibility for better modelling of the shear response. The back or shift stress p_α consists of two components: p_0, the thermodynamic force to which the dissipation is proportional; and p_b, the thermodynamic force conjugate to $d\varepsilon_v^p$ in the locked energy associated with the interparticle bonding. It is evident that bonding increases p_0 and makes p_b negative (release instead of accumulation of the locked energy). With $\alpha = 1$, $p_b = 0$, and p_0 defined based on remoulded consolidation states, the yield function reduces to the Cam-clay yield surface.

Following the Cam-clay approach, in the present model the plastic volumetric strain is used as the internal variable characterising the material fabric in remoulded states. An additional internal variable ξ_b is introduced to characterise bonding evolution. Therefore, as p_0 depends on both remoulded and bonding fabric, and p_b depends on the bonding fabric only, one has the functional dependences $p_0 = p_0(\varepsilon_v^p, \xi_b)$ and $p_b = p_b(\xi_b)$.

Flow rule

An associative flow rule holds in the dissipative stress space such that the dilatancy function

$$D = \frac{d\varepsilon_v^p}{|\delta\varepsilon_q^p|} = \frac{\partial f_D/\partial p_D}{|\partial f_D/\partial q_D|} = \frac{\tilde{M}^2 p_D}{|q_D|} = M^2\left[\alpha + (1-\alpha)\frac{2(p-p_b)}{p_0}\right]^2\frac{(p-p_b-p_0/2)}{|q|} \tag{25}$$

For convenience, the loading index is scaled such that

$$\delta\varepsilon_q^p = \langle L\rangle\frac{q}{|q|} \text{ and } d\varepsilon_v^p = \langle L\rangle D \tag{26}$$

Hardening and plastic modulus

The condition of consistency of the yield function (equation (24)) is

$$df = \frac{\partial f}{\partial p}dp + \frac{\partial f}{\partial q}dq + \frac{\partial f}{\partial p_0}\frac{\partial p_0}{\partial \varepsilon_v^p}d\varepsilon_v^p + \left(\frac{\partial f}{\partial p_0}\frac{\partial p_0}{\partial \xi_b} + \frac{\partial f}{\partial p_b}\frac{\partial p_b}{\partial \xi_b}\right)\delta\xi_b = 0 \tag{27}$$

Based on the assumption of incremental linearity, one has

$$\delta\xi_b = \langle L\rangle r_b \tag{28}$$

where r_b is in general a function of stress and internal variables. The size of the yield surface p_0 can be conceptually categorised into two parts, one due to the internal structure of the particle assemblage and the other due to the interparticle bonding. For remoulded soils $p_0 = p_\varepsilon$, and for bonded soil $p_0 = p_\varepsilon + p_\mu$, where $p_\mu = p_\mu(\xi_b)$ reflects the additional yielding strength contributed by bonding. With equations (26)$_{''>''>2}$ and (28), equation (27) can be rewritten in the standard form

$$df = \frac{\partial f}{\partial p}dp + \frac{\partial f}{\partial q}dq - \langle L\rangle K_p = 0 \tag{29}$$

where the plastic modulus K_p is given by

$$K_p = -\left[\frac{\partial f}{\partial p_0}\frac{\partial p_0}{\partial \varepsilon_v^p}D + \left(\frac{\partial f}{\partial p_0}\frac{\partial p_0}{\partial \xi_b} + \frac{\partial f}{\partial p_b}\frac{\partial p_b}{\partial \xi_b}\right)r_b\right] = -\left[\frac{\partial f}{\partial p_0}\frac{\partial p_\varepsilon}{\partial \varepsilon_v^p}D + \left(\frac{\partial f}{\partial p_0}\frac{\partial p_\mu}{\partial \xi_b} + \frac{\partial f}{\partial p_b}\frac{\partial p_b}{\partial \xi_b}\right)r_b\right] \tag{30}$$

Following the Cam-clay hardening law

$$p_\varepsilon\left(\varepsilon_v^p\right) = e^{(N - v_0^p + v_0\varepsilon_v^p)/(\lambda-\kappa)} \tag{31}$$

so that

$$\frac{\partial p_\varepsilon}{\partial \varepsilon_v^p} = \frac{v_0}{\lambda-\kappa}p_\varepsilon \tag{32}$$

where λ, κ and N are the familiar Cam-clay constants for the soil in remoulded states; and v_0 and v_0^p are the initial specific volume and its plastic part respectively.

The internal variable ξ_b reflects the bonding condition, and is proposed to be an accumulated plastic deformation

$$\xi_b = p_{atm}\int\sqrt{\frac{\delta\varepsilon_{ij}^p\delta\varepsilon_{ij}^p}{(p-p_b-p_0/2)^2}} = p_{atm}\int\sqrt{\frac{2(d\varepsilon_v^p)^2 + 9(\delta\varepsilon_q^p)^2}{6(p-p_b-p_0/2)^2}} \tag{33}$$

and its increment is given by

$$\delta\xi_b = p_{atm}\sqrt{\frac{2(d\varepsilon_v^p)^2 + 9(\delta\varepsilon_q^p)^2}{6(p - p_b - p_0/2)^2}} = \langle L\rangle \underbrace{p_{atm}\sqrt{\frac{2D^2+9}{6(p - p_b - p_0/2)^2}}}_{r_b} = \langle L\rangle r_b \tag{34}$$

It can be seen that, in the intact state, $\xi_b = 0$; and when the material approaches critical state with a zero dilatancy (refer to equation (25)), $\xi_b = \infty$, the bonding is completely destroyed. Therefore ξ_b can be viewed as a measure of bonding destructuration. It follows that p_μ can be expressed as an exponential function of ξ_b as

$$p_\mu = p_{\mu 0} e^{-a\{v_0/(\lambda-\kappa)\}\xi_b} \tag{35}$$

where $p_{\mu 0}$ is the initial (intact) value of p_μ, and a is a positive material constant controlling the rate of destructuration. Equations (33) and (35) guarantee that the cohesion is destroyed at critical states. The material constant a affects the failure brittleness in cases where significant cohesion is left over during shearing.

Because p_μ and p_b both originate from the effect of interparticle bonding, they are homogeneously related. For simplicity, the relation is assumed to be linear as well (Yu *et al.*, 2007), so that

$$p_b = \left(\frac{p_{b0}}{p_{\mu 0}}\right) p_\mu \tag{36}$$

where p_{b0} and $p_{\mu 0}$ are the initial values of p_b and p_μ. Based on equations (35) and (36), one has

$$\frac{\partial p_\mu}{\partial \xi_b} = -a\frac{v_0}{\lambda-\kappa} p_\mu \text{ and } \frac{\partial p_b}{\partial \xi_b} = -a\frac{v_0}{\lambda-\kappa} p_b \tag{37}$$

Substituting equations (32), (34) and (37) into equation (30) yields

$$K_p = -\left[\frac{\partial f}{\partial p_0}\frac{v_0 p_\varepsilon D}{\lambda-\kappa} - \frac{a v_0}{\lambda-\kappa}\left(\frac{\partial f}{\partial p_0} p_\mu + \frac{\partial f}{\partial p_b} p_b\right) \times p_{atm}\sqrt{\frac{2D^2+9}{6(p - p_b - p_0/2)^2}}\right] \tag{38}$$

in which the partial derivatives $\partial f/\partial p_0$ and $\partial f/\partial p_b$ have been given by equations $(24)_{3,4}$.

Elasto-plastic stiffness

In triaxial space, the incremental stress–strain relationship equation (13) is reduced to

$$\begin{Bmatrix} dp \\ dq \end{Bmatrix} = \begin{bmatrix} \Lambda_{11} & \Lambda_{12} \\ \Lambda_{21} & \Lambda_{22} \end{bmatrix} \begin{Bmatrix} d\varepsilon_v \\ d\varepsilon_q \end{Bmatrix} \tag{39}$$

with

$$\begin{bmatrix} \Lambda_{11} & \Lambda_{12} \\ \Lambda_{21} & \Lambda_{22} \end{bmatrix} = \begin{bmatrix} K & 0 \\ 0 & 3G \end{bmatrix} - \frac{h(L)}{KD\frac{\partial f}{\partial p} + 3G\frac{\partial f}{\partial q}\frac{q}{|q|} + K_p} \begin{bmatrix} K^2 D\frac{\partial f}{\partial p} & 3KGD\frac{\partial f}{\partial q} \\ 3KG\frac{\partial f}{\partial p}\frac{q}{|q|} & 9G^2\frac{\partial f}{\partial q}\frac{q}{|q|} \end{bmatrix} \tag{40}$$

in which the partial derivatives $\partial f/\partial p$ and $\partial f/\partial q$ have been given in equations $(24)_{1,2}$, and the loading index can be calculated by

$$L = \frac{K\frac{\partial f}{\partial p} d\varepsilon_v + 3G\frac{\partial f}{\partial q} d\varepsilon_q}{KD\frac{\partial f}{\partial p} + 3G\frac{\partial f}{\partial q}\frac{q}{|q|} + K_p} \tag{41}$$

As shown in equation (40), the stiffness matrix is generally non-symmetric, which reveals the nature of non-associative flow rule in the actual stress space.

CALIBRATION OF MODEL CONSTANTS

There are seven material constants in the present model. Five of them (λ, κ, M, N, ν) are traditional parameters appearing in the Cam-clay models. The constant α is used to modify the shape of the yield surface for better prediction of shear response (Collins & Kelly, 2002). The only new material constant introduced in the present model is a, which controls bonding evolution. In addition, the initial values of the internal variables p_ε, p_b and p_μ are to be specified in reference to the intact state of the soil. The five traditional material constants (λ, κ, M, N, ν) can be calibrated based on conventional triaxial tests on remoulded specimens. The procedure is standard, and will not be elaborated further here. α defines the shape of the yield surface: thus it can be determined in an optimal sense by gathering a set of yield points from triaxial tests along different p–q paths. α affects the relative spacing in e–$\ln p$ space among virgin compression lines of different stress ratios.

The initial value of p_ε can be determined based on equation (31) by setting $\varepsilon_v^p = 0$, such that

$$p_{\varepsilon 0} = e^{(N - v_0^p)/(\lambda-\kappa)} \tag{42}$$

where v_0^p is the specific volume of the intact soil specimen at zero effective confining pressure. The initial values of p_b and p_μ (p_{b0} and $p_{\mu 0}$) can be determined simultaneously from two tests on intact specimens: an isotropic compression test and an unconfined compression drained test (the lateral effective stress is zero). Referring to Fig. 4, the two tests result in two yielding stress values: p_{yield} and $q_f = 3p_f$, where

$$p_{yield} = p_{\varepsilon 0} + p_{\mu 0} + p_{b0} \tag{43}$$

and by invoking the yield function (equation (23)), one has

$$M^2\left[\alpha + (1-\alpha)\frac{2(q_f/3 - p_{b0})}{p_{\varepsilon 0} + p_{\mu 0}}\right]^2 \times \left[\left(\frac{q_f}{3} - p_{b0}\right)^2 - \left(\frac{q_f}{3} - p_{b0}\right)(p_{\varepsilon 0} + p_{\mu 0})\right] + q_f^2 = 0 \tag{44}$$

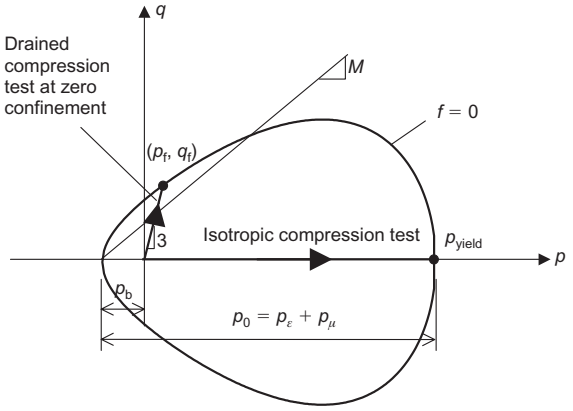

Fig. 4. Yielding in an isotropic compression test and unconfined drained compression tests

By solving equations (43) and (44) simultaneously, we obtain $p_{\mu 0}$ and p_{b0}.

The material constant a affects the rate of destructuration during loading, which can be determined, again in an optimal sense, by fitting either isotropic or K_0 consolidation data on intact specimens, as illustrated later in Fig. 5.

MODEL RESPONSES

Model responses under different stress paths are presented to demonstrate the novel features of the proposed model. Fig. 5 shows the model responses to isotropic compression with a set of representative model constants. In the figure, curve 1 shows the response of a remoulded (unbonded) soil, and curves 2 to 5 show the responses of the bonded soil with different combinations of $p_{\mu 0}$, p_{b0} and a. The impact of each parameter is demonstrated. It can be seen that the bonded soil exhibits a stiffer response up to a higher stress until destructuration occurs, and the yield stress is controlled by the values of $p_{\mu 0}$ and p_{b0}. As shown in the figure, the model constant a affects the rate of destructuration. However, the overall response of isotropic compression is rather insensitive to this parameter.

Figure 6 shows the response of drained triaxial shearing tests on the same hypothetical soil with different initial bonds. The shear starts from an overconsolidated state (point

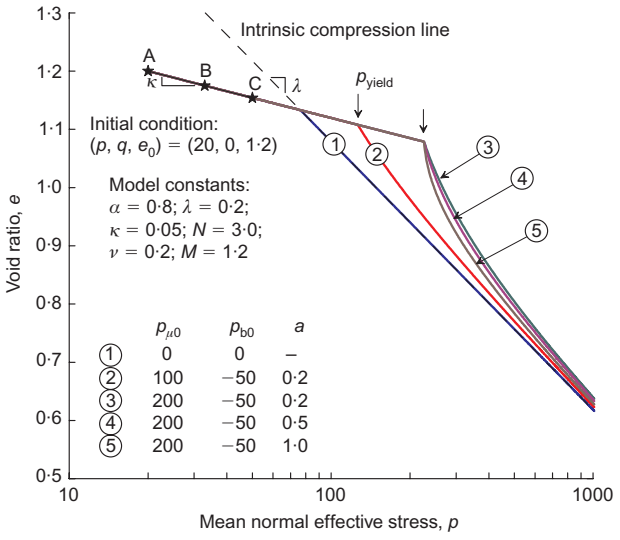

Fig. 5. Influence of a and p_μ on isotropic compression

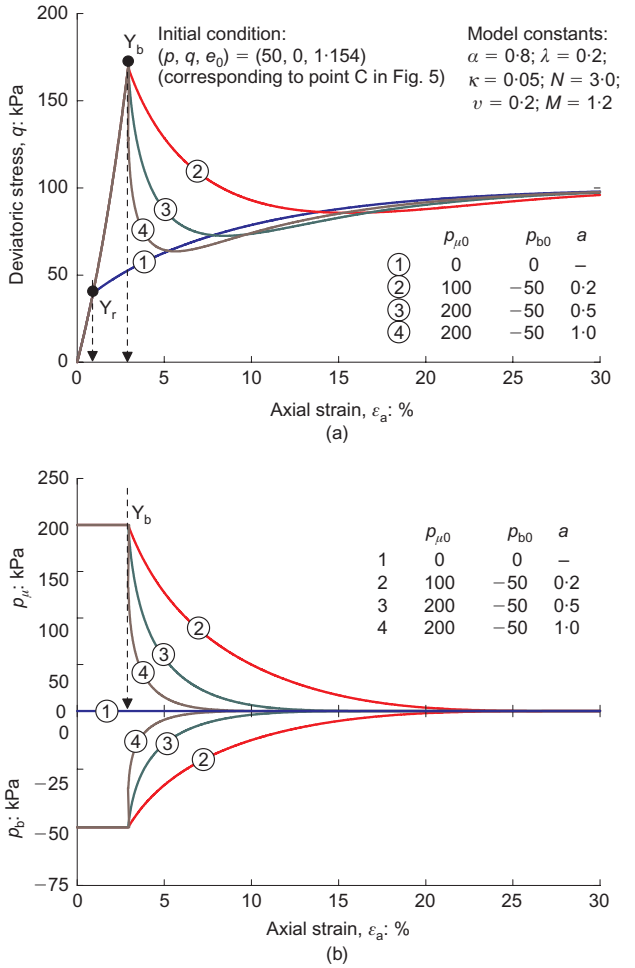

Fig. 6. Effect of a and p_μ on a drained compression test: (a) stress–strain response; (b) evolution of p_μ and p_b

C; refer to Fig. 5). Fig. 6(a) shows the stress–strain response, and Fig. 6(b) illustrates the evolution of bonding in terms of p_μ and p_b against the axial strain. Curve 1 shows the behaviour of the remoulded soil (i.e. $p_\mu = 0$ and $p_b = 0$), where the material yields at Y_r. Curves 2 to 4 show the responses of the bonded specimens. The bonded specimens first yield at Y_b, which is noticeably higher than Y_r, and this is then followed by softening. The high yield strength is due to the enlarged and shifted yield surface characterised by the parameters p_μ and p_b. Different rates of strain-softening are associated with different values of a, and the response is rather sensitive to this parameter. This is contrary to the destructuration behaviour under isotropic compression shown in Fig. 5. As shown in Fig. 6(b), a higher a gives a markedly faster softening response (a higher destructuration rate). As shear continues, both p_μ and p_b approach zero, and the ultimate shear strength becomes the same as that for the remoulded specimen, indicating that the bonded soil has been tuned to be fully remoulded, and the strength is governed only by the frictional properties of the material and the confining stress.

According to equations (34) to (37), an abrupt bond destructuration may occur at $p = p_b + p_0/2$, as it makes ξ_b approach infinity, resulting in $p_\mu = 0$ and $p_b = 0$ almost instantaneously. Fig. 7 shows such a response under drained shear. In the figure shear starts from point B (refer to Fig. 5). While the remoulded soil yields at Y_r, the bonded specimen starts to yield at a much higher stress Y_b. As shown in Fig. 7(b), Y_b happens to satisfy the stress condition

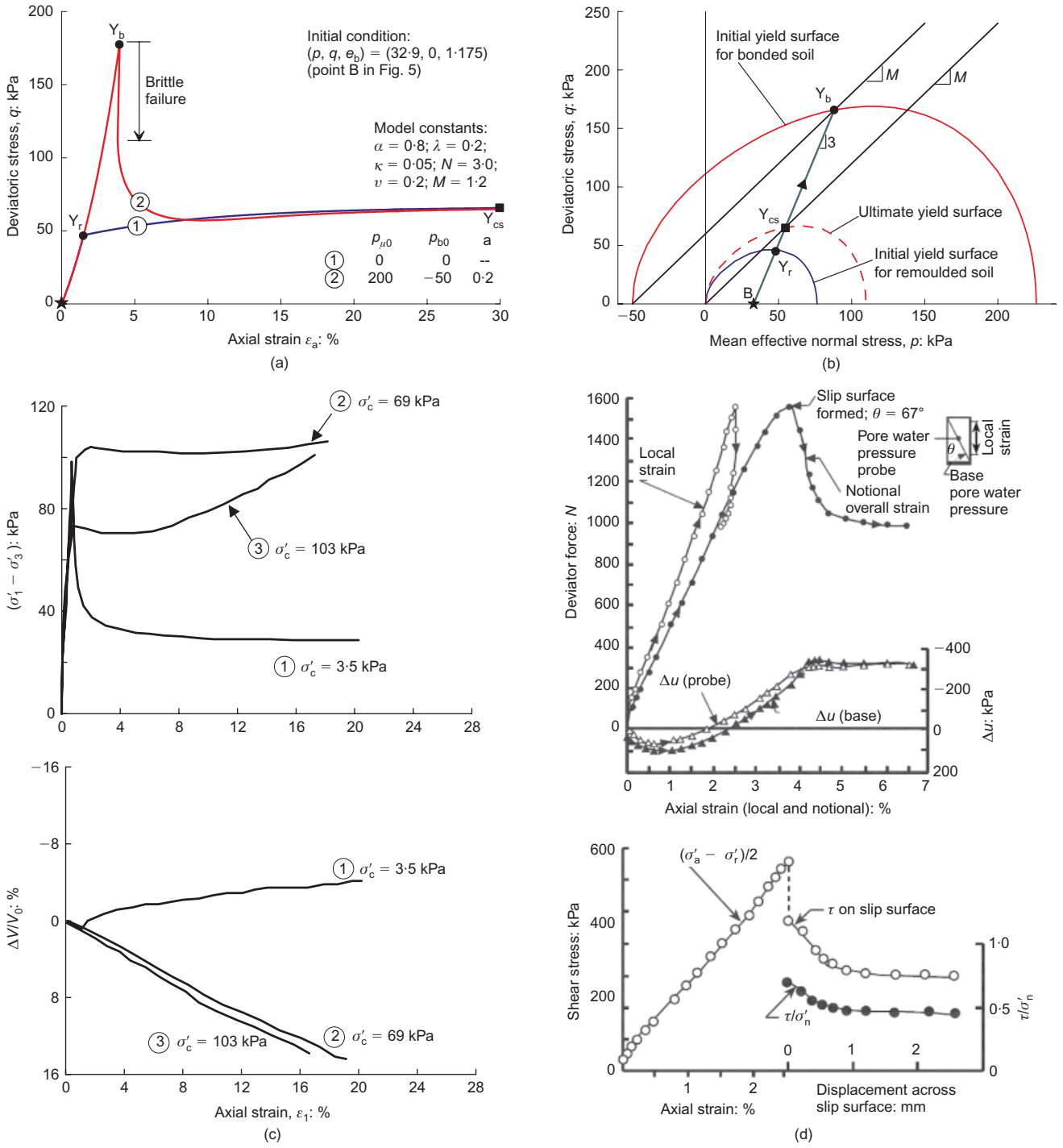

Fig. 7. Brittle failure of a natural soil during shearing: (a) model stress–strain response in drained test; (b) evolution of yield surface; (c) Saint Vallier clay (adopted from Lefebvre, 1970); (d) Todi clay (adopted from Burland, 1990)

$p = p_b + p_0/2$, resulting in an abrupt destructuration (a brittle failure), as seen in Fig. 7(a). Figs 7(c) and 7(d) show the brittle rupture of natural soils, Saint Vallier clay and Todi clay adopted from Lefebvre (1970) and Burland (1990) respectively, upon shearing. A very distinct peak and post-peak softening can be identified. One can clearly see that the model is able qualitatively to replicate such brittle rupture response of natural soils. Similar to Fig. 6, both bonded and remoulded soil give the same critical-state strength (Y_{cs}) at large strains, in agreement with the observation by Burland *et al.* (1996) that the post-rupture Mohr–Coulomb strength line is close to the intrinsic critical-state failure line.

COMPARISON WITH EXPERIMENTS

Attempts have been made to simulate the test results of natural clays reported in the literature. Fig. 8 shows the response of two natural soils (Bothkennar clay and Pisa clay respectively) to one-dimensional compression (Smith *et al.*, 1992; Callisto & Calabresi, 1998). The 'undisturbed' intact samples bear higher yield stresses than the reconstituted ones, and the destructuration process can be seen upon continuous loading. The experimental results are simulated with the model constants shown in the figure. The simulated response is in good agreement with the experimental data.

Figure 9 shows test data on an intact stiff clay (Pietrafitta clay). The tests include one-dimensional consolidation and

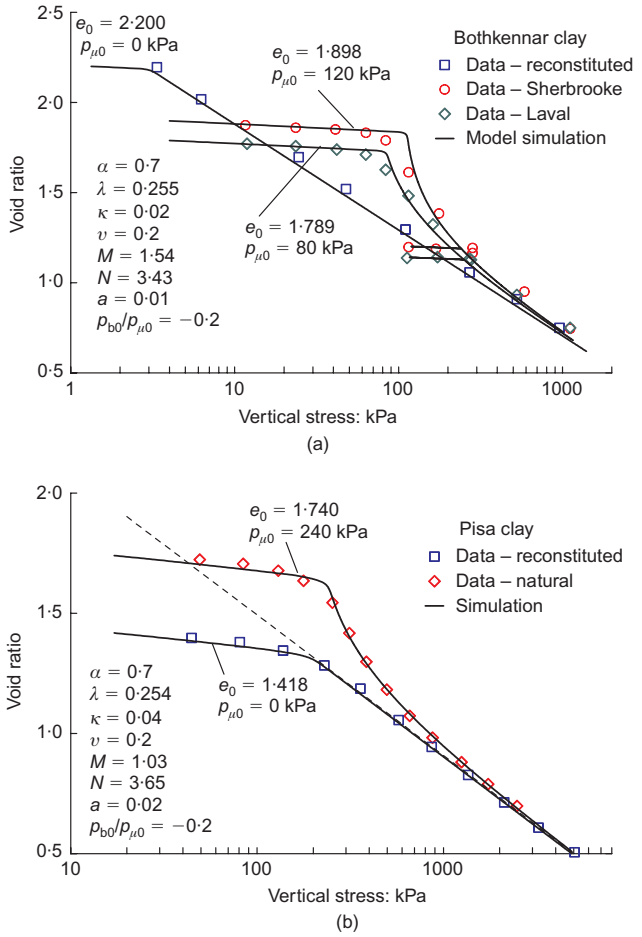

Fig. 8. Experimental results and model simulations on one-dimensional consolidation tests: (a) Bothkennar clay (data from Smith *et al.*, 1992); (b) Pisa clay (data from Callisto & Calabresi, 1998)

triaxial compression shearing (Burland *et al.*, 1996). The corresponding model simulations are also shown in the figure. The basic model constants such as M, N, λ and κ can be found in Burland's original paper. Poisson's ratio ν is taken as 0·2, which is considered as typical. The model constants are summarised in Table 1, in which the constant a is calibrated on an optimal basis. Fig. 9(a) shows both the experimental and simulated one-dimensional consolidation response of the soil. Good agreement can be readily seen. Figs 9(b) and 9(c) summarise the soil responses during undrained shear (CU test). The number attached to each curve denotes the initial confining pressure prior to shearing. It can be seen that, as the confining pressure increases, the soil becomes more contractive (reflected by an increasing pore pressure change). This trend is well captured by the model. It can also be seen that the model reproduced the softening response shown in all the tests, owing to bond destructuration. In the undrained stress paths, as shown in Fig. 9(c), experimental data are shown up to the peak only; post-peak modelling responses are represented by dotted lines. Fig. 9(d) shows the drained shear results, both experimental and simulated. In the figure, CD53 denotes the conventional drained shear test with an effective cell pressure of 53 kPa, and CP53 and CP96 denote the constant-p' shear tests with $p' = 53$ and 96 kPa respectively. The simulation broadly captures the trends of the response.

Table 1. Summary of model constants for Pietrafitta clay (Burland *et al.*, 1996)

Conventional parameters		Newly introduced parameters	
υ	0·2	α	0·8
λ	0·227	a	0·16
κ	0·051		
N	3·490		
M	1·13		

CONCLUSION

This paper demonstrates the development of a thermodynamically consistent constitutive model for natural soils with bonds. Upon plastic loading, the bonds may break and liberate certain accumulated locked energy. The novel aspect of the present model is that it explicitly models the evolution of the thermodynamic force conjugate to plastic volumetric deformation in locked energy such that the bond-associated locked energy is completely released at critical states. The model contains seven model constants, of which five are the conventional Cam-clay parameters. Two additional constants are used to improve the shape of the yield surface, and to characterise the rate of bond destructuration. The performance of the model is demonstrated by numerical examples and by comparisons of the model simulation with test results in the literature.

ACKNOWLEDGEMENTS

The first author would like to acknowledge the Fundo para o Desenvolvimento das Ciências e da Tecnologia (FDCT), Macau SAR government (Grant No. 013/2007/A1) and the Research Committee, University of Macau (Grant No. RG053/06–07S/YWM/FST) for their financial assistance at the initial stage of this research.

NOTATION

a material constant
c parameters denoting cohesion in Yu *et al.* (2007)
D dilatancy
e void ratio
f yield function in actual stress space
f_D yield function in dissipative stress space
G elastic shear modulus
$\mathcal{H}$ material internal structure
h Heaviside function
K elastic bulk modulus
K_p plastic modulus
K_0 coefficient of lateral earth pressure at rest
L loading index
M classical Cam-clay constant
$\bar{M}$ modified version of Cam-clay constant M
N material constant
p mean normal stress
p_{atm} atmospheric pressure
p_b mean back stress associated with bonding
p_{b0} initial value of p_b
p_D, q_D dissipative stresses
p_f yield mean stress in drained compression test
p_{yield} yield mean stress in isotropic compression test
p_α, q_α back stresses
p_ε size of yield surface for remoulded soil
p_μ additional size of yield surface due to bonding
$p_{\mu 0}$ initial value of p_μ
p_0 size of yield surface in actual stress space
Q heat entering an element
q deviatoric stress
q_f yield deviatoric stress in drained compression test
r general functions of stress and material's internal structure

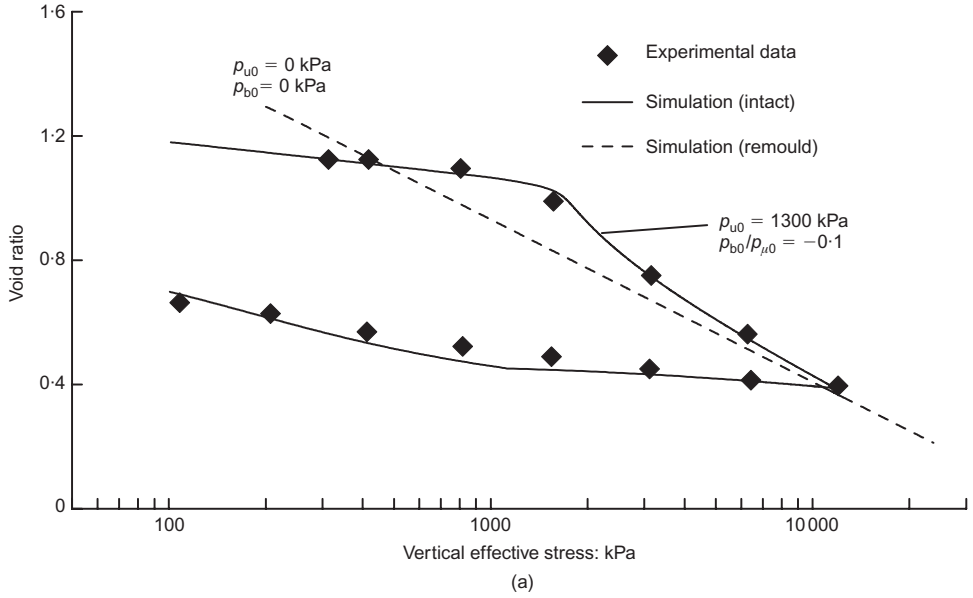

(a)

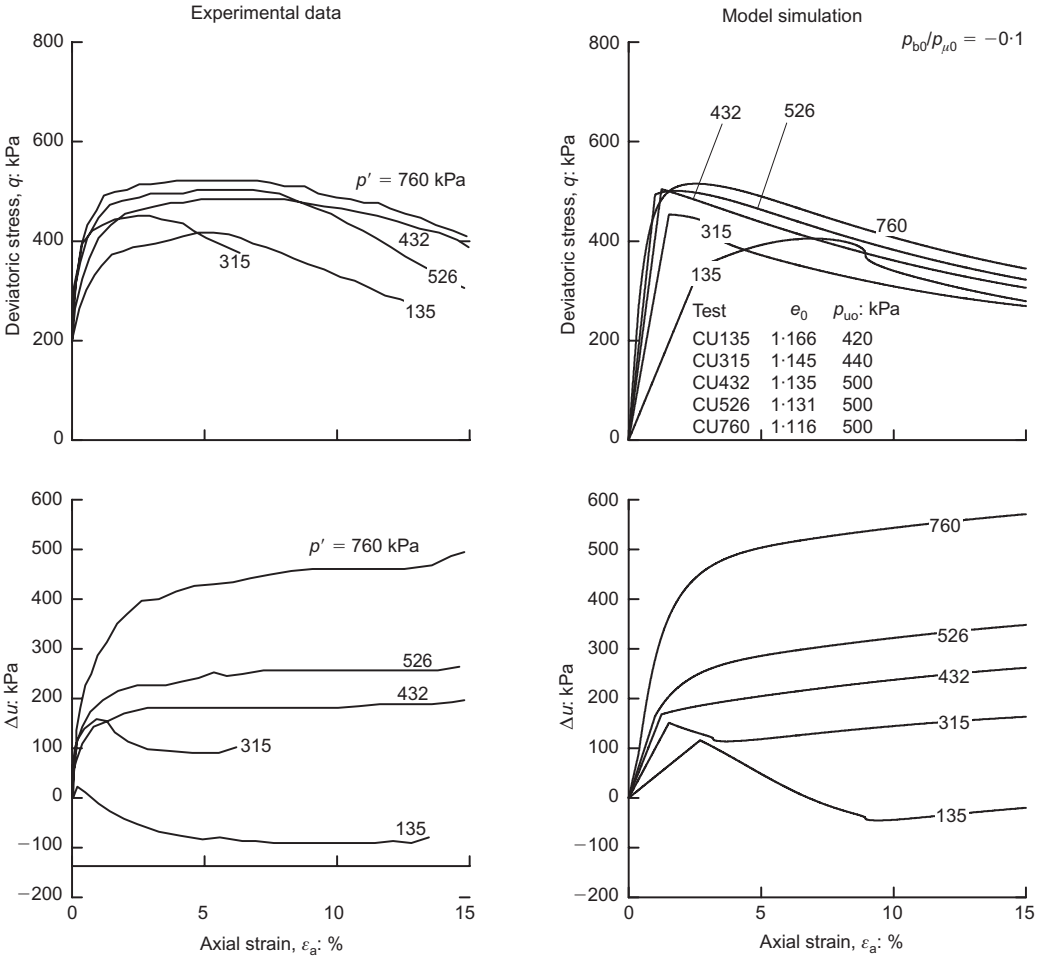

(b)

Fig. 9. Comparison of results for Pietrafitta clay (Burland *et al.*, 1996): (a) one-dimensional compression; (b) undrained shearing;

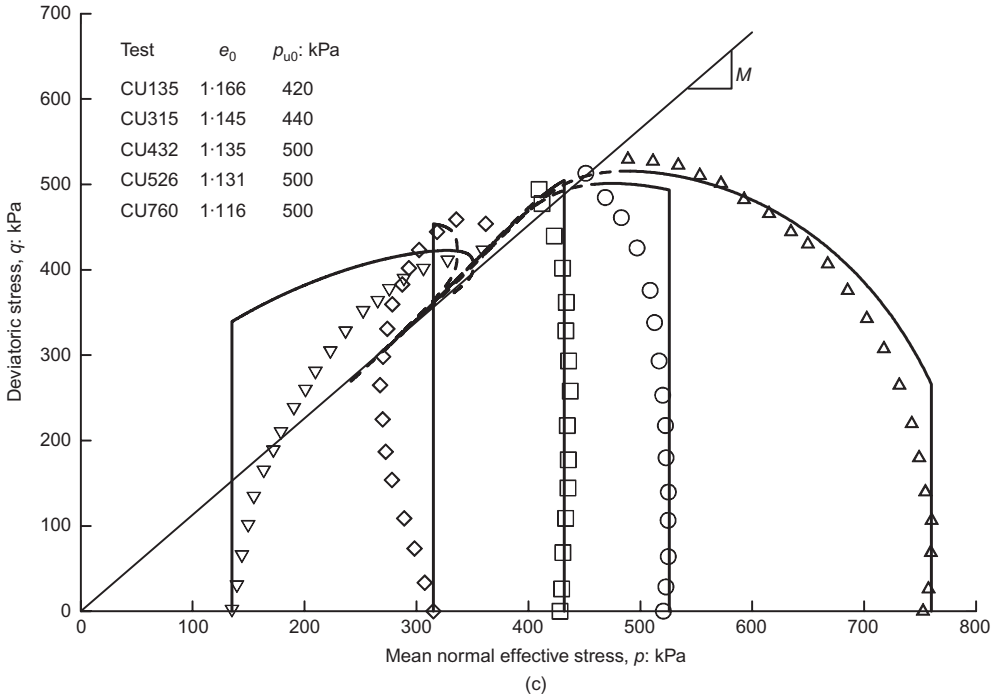

(c)

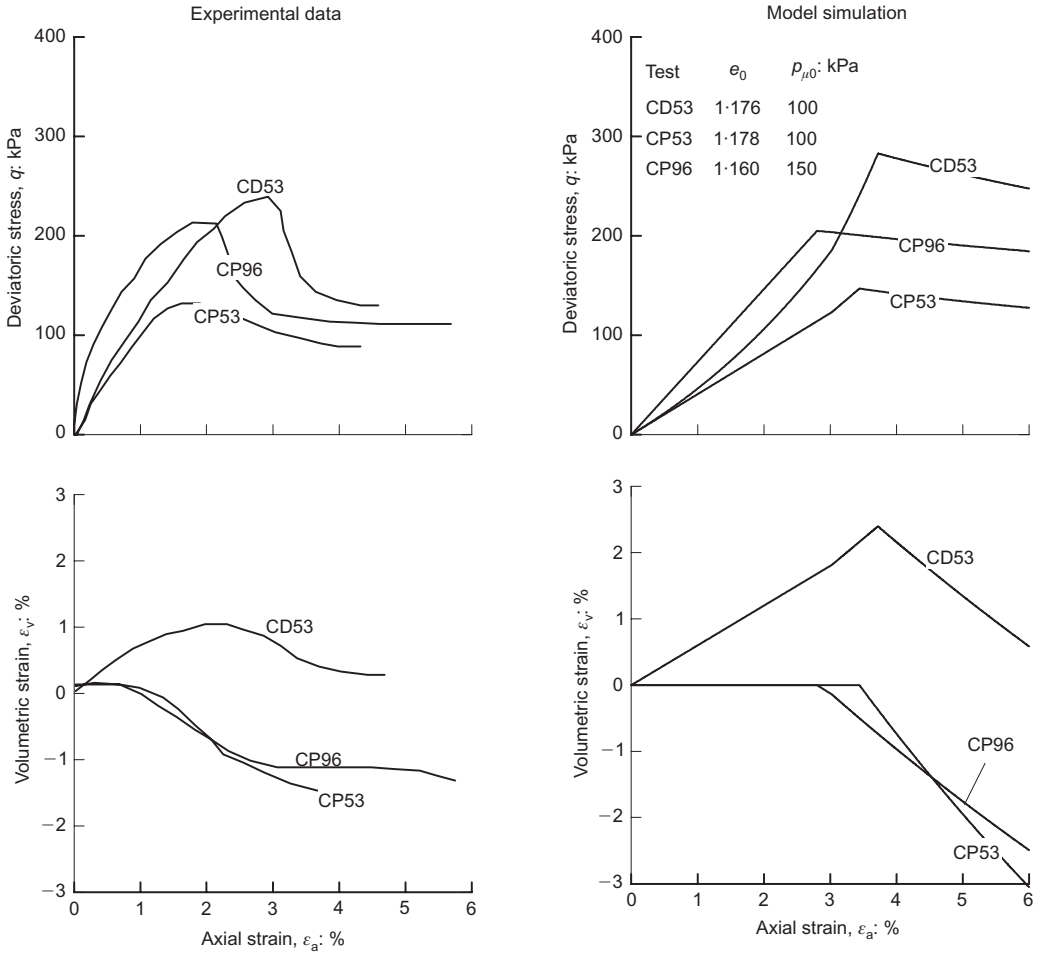

(d)

Fig. 9. (c) stress path; (d) drained shearing

r_b function related to stress and bonded internal structure
s sensitivity parameter; entropy
$\dot{s}$ rate of change of sensitivity parameter
u internal heat energy
v_0 initial specific volume
v_0^p plastic part of initial specific volume
Y_b first yield for bonded soil in triaxial drained shear
Y_{cs} yield point at critical state in triaxial drained shear
Y_r first yield for remoulded soil in triaxial drained shear
α shape of yield function
$\boldsymbol{\alpha}$ back or shifted stress
γ entropy production
ε_a axial strain
ε_q deviatoric strain
ε_r radial strain
ε_v volumetric strain
ε_v^e elastic volumetric strain
ε_v^p plastic volumetric strain
$\delta\varepsilon_q^p$ plastic deviatoric strain increment
$d\varepsilon_v^p$ plastic volumetric strain increment
$\boldsymbol{\varepsilon}$ strain
$\boldsymbol{\varepsilon}^e$ elastic strain
$\boldsymbol{\varepsilon}^p$ plastic strain
θ absolute temperature
κ, λ, ν material constants
ξ_b measure of bond destructuration
σ_a axial stress
σ_r radial stress
$\boldsymbol{\sigma}$ effective stress
$\boldsymbol{\sigma}_D$ dissipative stress
ϕ dissipation
ψ Helmholtz free energy

REFERENCES

Baudet, B. & Stallebrass, S. (2004). A constitutive model for structured clays. *Géotechnique* **54**, No. 4, 269–278, **doi**: 10.1680/geot.2004.54.4.269.

Burland, J. B. (1990). On the compressibility and shear strength of natural clays. *Géotechnique* **40**, No. 3, 329–378, **doi**: 10.1680/geot.1990.40.3.329.

Burland, J. B., Rampello, S., Georgiannou, V. N. & Calabresi, G. (1996). A laboratory study of the strength of four stiff clays. *Géotechnique* **46**, No. 3, 491–514, **doi**: 10.1680/geot.1996.46.3.491.

Callisto, L. & Calabresi, G. (1998). Mechanical behaviour of a natural soft clay. *Géotechnique* **48**, No. 4, 495–513, **doi**: 10.1680/geot.1998.48.4.495.

Collins, I. F. & Houlsby, G. T. (1997). Application of thermomechanical principles to the modelling of geotechnical materials. *Proc. R. Soc. London Ser. A* **453**, 1975–2001.

Collins, I. F. & Kelly, P. A. (2002). A thermomechanical analysis of a family of soil models. *Géotechnique* **52**, No. 7, 507–518, **doi**: 10.1680/geot.2002.52.7.507.

Cotecchia, F. & Chandler, R. J. (2000). A general framework for the mechanical behaviour of clays. *Géotechnique* **50**, No. 4, 431–447, **doi**: 10.1680/geot.2000.50.4.431.

Gasparre, A., Nishimura, S., Coop, M. R. & Jardine, R. J. (2007). The influence of structure on the behaviour of London Clay. *Géotechnique* **57**, No. 1, 19–31, **doi**: 10.1680/geot.2007.57.1.19.

Houlsby, G. T. & Puzrin, A. M. (2000). A thermomechanical framework for constitutive models for rate-independent dissipative materials. *Int. J. Plasticity* **16**, 1017–1047.

Lefebvre, G. (1970). *Contribution à l'étude de la stabilité des pentes dans les argiles cimenteés*. PhD thesis, Université Lavel, Québec.

Leroueil, S. & Vaughan, P. R. (1990). The general and congruent effects of structure in natural soils and weak rocks. *Géotechnique* **40**, No. 3, 467–488, **doi**: 10.1680/geot.1990.40.3.467.

Li, X. S. (2007a). Thermodynamics-based constitutive framework for unsaturated soils. 1: Theory. *Géotechnique* **57**, No. 5, 411–422, **doi**: 10.1680/geot.2007.57.5.411.

Li, X. S. (2007b). Thermodynamics-based constitutive framework for unsaturated soils. 2: A basic triaxial model. *Géotechnique* **57**, No. 5, 423–435, **doi**: 10.1680/geot.2007.57.5.423.

Rice, J. R. (1971). Inelastic constitutive relations for solids: an internal variable theory and its application to metal plasticity. *J. Mech. Phys. Solids* **19**, No. 6, 433–455.

Roscoe, K. H. & Burland, J. B. (1968). On the generalized stress–strain behaviour of wet clays. In *Engineering plasticity* (eds J. Heyman and F. A. Leckie), pp. 535–609. Cambridge: Cambridge University Press.

Roscoe, K. H. & Schofield, A. N. (1963). Mechanical behaviour of an idealized 'wet' clay. *Proc. 2nd Eur. Conf. Soil Mech. Found. Engng, Wiesbaden* **1**, 47–54.

Roscoe, K. H., Schofield, A. N. & Wroth, W. P. (1958). On the yielding of soils. *Géotechnique* **8**, No. 1, 22–53, **doi**: 10.1680/geot.1958.8.1.22.

Schofield, A. N. (1998). *The 'Mohr–Coulomb' error*. Cambridge University Engineering Department, Division D Soil Mechanics Group Technical Report Number 305.

Schofield, A. N. (2005). *Disturbed soil properties and geotechnical design*. London: Thomas Telford.

Schofield, A. N. (2006). Interlocking, and peak and design strengths. *Géotechnique* **56**, No. 5, 357–358, **doi**: 10.1680/geot.2006.56.5.357.

Schofield, A. N. & Wroth, C. P. (1968). *Critical state soil mechanics*. London: McGraw-Hill.

Smith, P. R., Jardine, R. J. & Hight, D. W. (1992). The yielding of Bothkennar clay. *Géotechnique* **42**, No. 2, 257–274, **doi**: 10.1680/geot.1992.42.2.257.

Taylor, D. W. (1948). *Fundamentals of soil mechanics*. New York: Wiley & Sons.

Yu, H. S., Tan, S. M. & Schnaid, F. (2007). A critical state framework for modelling bonded geomaterials. *Geomech. Geoengng* **2**, No. 1, 61–74.

Ziegler, H. (1983). *An introduction to thermomechanics.* Amsterdam: North-Holland.